Hydrology and Earth System Sciences Discussions

Sensitivity of point scale runoff predictions to rainfall resolution

A. J. Hearman and C. Hinz

School of Earth and Geographical Sciences, University of Western Australia, Perth, Australia

Correspondence to: C. Hinz (christoph.hinz@uwa.edu.au)

HESSD

3, 3517–3556, 2006

Sensitivity of runoff predictions to rainfall resolution

A. J. Hearman and C. Hinz

Title Page

Abstract	Introduction
Conclusions	References
Tables	Figures

| ◄◄ | ►► |
| ◄ | ► |

Back | Close

Full Screen / Esc

Printer-friendly Version

Interactive Discussion

EGU

Abstract

This paper investigates the effects of using non-linear, high resolution rainfall, compared to time averaged rainfall on the triggering of hydrologic thresholds and therefore model predictions of infiltration excess and saturation excess runoff. The bounded random cascade model, parameterized to south western Australian rainfall, was used to scale rainfall intensities at various time resolutions ranging from 1.875 min to 2 h. A one dimensional, conceptual rainfall partitioning model was used that instantaneously partitions water into infiltration excess, infiltration, storage, deep drainage, saturation excess and surface runoff, where the fluxes into and out of the soil store are controlled by thresholds. For example, saturation excess is triggered when the soil water content reaches the storage capacity threshold. The results of the numerical modelling were scaled by relating soil infiltration properties to soil draining properties, and inturn, relating these to average storm intensities. By relating maximum soil infiltration capacities to saturated drainage rates (f^*), we were able to split soils into two groups; those where all runoff is a result of infiltration excess alone ($f^* \leq 0.2$) and those susceptible to both infiltration excess and saturation excess runoff ($f^* > 0.2$). For all soil types, we related maximum infiltration capacities to average storm intensities (k^*) and were able to show where model predictions of infiltration excess were most sensitive to rainfall resolution (ln $k^* = 0.4$) and where using time averaged rainfall data can lead to an under prediction of infiltration excess and an over prediction of the amount of water entering the soil (ln $k^* > 2$). For soils susceptible to both infiltration excess and saturation excess, total runoff sensitivity was scaled by relating saturated drainage rates to average storm intensities (g^*) and parameter ranges where predicted runoff was dominated by infiltration excess or saturation excess depending on the resolution of rainfall data was determined (ln $g^* < 2$). Infiltration excess predicted from high resolution rainfall is short and intense, whereas saturation excess produced from low resolution rainfall is more constant and less intense. This has important implications for the accuracy of current hydrological models that use time averaged rainfall under these soil and rainfall condi-

tions and predictions of further thresholds such as erosion. It offers insight into areas where the understanding of the dynamics of high resolution rainfall is required and a means by which we can improve our understanding of the way variations in rainfall intensities within a storm relate to hydrological thresholds and model predictions.

1 Introduction

Traditionally, hydrological models use steady state rainfall or time averaged rainfall data. There have been a number of studies that have suggested that including the storminess or peaks in rainfall intensities throughout a storm may affect our modelled results. Wainwright and Parsons (2002) showed that overland flow models that use mean rainfall intensity under predict runoff. Bronstert and Bardossy (2003) found that 1 hour resolution clearly underestimated runoff volumes attributed to Hortonian overland flow (infiltration excess). Mertens et al. (2002) compared simulated surface runoff using HYDRUS-1D and 10 min rainfall data to results using the Soil Conservation Service (SCS) runoff curve-number method and found that depending on the season or storm intensity, the curve-number method overestimates surface runoff (winter) or underestimates surface runoff (summer). Milly (1994) suggested the inclusion of intra-seasonal variability (storminess) of precipitation may be a reason for their under prediction of mean annual runoff by 30% when looking at seasonal distributions of water and energy on the mean annual water balance. These studies highlight the need for a better understanding of how rainfall resolution affects our predictions of runoff and the soil and rainfall conditions in which high resolution rainfall is most important for accurate model predictions.

A limitation of these studies and other ecological and hydrological modelling has been the lack of high resolution rainfall as model inputs. The collection of such data is costly and time consuming and even if this data is available, there is still uncertainty as to how well a previous rainfall pattern will represent future rainfall patterns. This has lead to the use of stochastic simulation of rainfall and analysis of the statistical

EGU

properties of hydrological modelling. For this reason, in the last 20 years there have been many studies into the transformation of available rainfall data from one scale to another (see Lovejoy and Schertzer, 2005 for an overview). All disaggregation methods are based on describing the variability at one scale in relation to the variability

5   at another scale. One of the most prevalent and promising methods is the use of multifractal random cascades which are able to reproduce the statistical properties of non-extreme rainfall events as well as extreme rainfall events (Veneziano et al., 1996, Over and Gupta, 1996, Menabde et al., 1997). In this paper we use the bounded random cascade approach described by Menabde and Sivapalan (2000). This model

10 has been parameterized to Australian rainfall in Melbourne (Menabde and Sivapalan, 2000) and also in south-western Australian (Hipsy et al., 2003). In this paper we use a single set of rainfall parameters (south-western Australia) as an illustration of a method to determine the soil, storm relationships most sensitive to rainfall resolution when predicting runoff for this particular region. The paper sets out to understand and determine

15 the effect of averaging rainfall data on the triggering of runoff thresholds and not the probability each event occurs.

   Whilst using complex rainfall as input, we kept our hydrological model as simple as possible, using a lumped parameter, bucket model. Wainwright and Parsons (2002) in their investigations of temporal variations in rainfall on runoff predictions also used a

20 single water balance storage model, similar to that of Kirkby (1978). Kirkby et al. (2005) compared this simple bucket model for infiltration excess to the Green-Ampt model for individual storm events and found that "*the major storm rainfall-runoff trajectories were approximately followed*" (pp. 144). There are numerous examples of the use of simple lumped storage representations of surface hydrology. Some of which include Milly

25 (1994), Kirkby and Cox (1995), Farmer et al. (2003) and Woods (2003). It is this minimalist, process based approach that we wish to adopt in our attempts to investigate how using rainfall measured at various time scales will influence the triggering of runoff thresholds. The results presented in this paper remain at the point scale because a prerequisite for predictions on a larger hill slope scale is a clear and accurate under-

Sensitivity of runoff predictions to rainfall resolution

A. J. Hearman and
C. Hinz

EGU

standing of the processes at the point scale. "*Even at the point scale there is much that remains to be learned about how best to represent the dynamic characteristics of infiltration and surface runoff generation*" (Beven, 2002, pp. 80).

This study aims to expand on previous research in this area in a number of ways.
Firstly, by looking at two different mechanisms of runoff generation, infiltration excess and saturation excess and how rainfall resolution may impact predictions of the mechanism dominating runoff generation. This modelling approach not only sets out to investigate differences in amounts of infiltration excess and saturation excess but also the dynamics, including maximum intensities, frequency processes are triggered and the time throughout a storm each process is active. Secondly, it quantifies the effects of rainfall resolution on runoff generation and identifies rainfall and soil conditions in which model predictions are most sensitive to rainfall resolution. This study has important implications for the accuracy of current hydrological models. It offers insight into areas where the understanding of the dynamics of high resolution rainfall is required and a means by which we can improve our understanding of the way variations in rainfall intensities within a storm relate to hydrological thresholds and model predictions.

2   Methods

2.1   Conceptual Model

A one dimensional, conceptual bucket model was developed that instantaneously partitions rainfall into infiltration excess (q_i), infiltration (p_{soil}), soil storage (w_{soil}), soil drainage (q_{ss}) and matrix saturation excess (q_{sat}) in a similar fashion to (Woods, 2003). Fluxes into and out of the soil store are controlled by simple thresholds, infiltration capacity (k_{soil}), field capacity (θ_{fc}) and matrix saturation (θ_{sat}). See Fig. 1.

We use a very simple maximum infiltration capacity threshold controlling the amount of water entering the soil profile. This is in the same form as the classic Horton overland flow model (Horton, 1933). The input of water to the soil profile is represented as an

Sensitivity of runoff predictions to rainfall resolution

A. J. Hearman and
C. Hinz

Title Page

Abstract	Introduction
Conclusions	References
Tables	Figures

◄   ►

Back   Close

Full Screen / Esc

Printer-friendly Version

Interactive Discussion

EGU

intensity over time ($p_{\text{soil}}(t)$). If the rainfall intensity ($p_{\text{rain}}(t)$) exceeds the infiltration capacity (k_{soil}), input is then equal to the infiltration capacity (k_{soil}):

$$p_{\text{soil}}(t) = \begin{cases} p_{\text{rain}}(t) & \text{if } p_{\text{rain}}(t) < k_{\text{soil}} \\ k_{\text{soil}}(t) & \text{if } p_{\text{rain}}(t) > k_{\text{soil}} \end{cases} \tag{1}$$

The remaining water becomes infiltration excess (q_i):

$$q_i(t) = \begin{cases} 0 & \text{if } p_{\text{soil}}(t) < k_{\text{soil}} \\ (p_{\text{soil}}(t) - k_{\text{soil}}) & \text{if } p_{\text{soil}}(t) > k_{\text{soil}} \end{cases} \tag{2}$$

Drainage (q_{ss}) occurs when the soil storage reaches a critical threshold (field capacity, θ_{fc}). (Struthers et al., 2006)

$$q_{ss}(t) = \begin{cases} 0 & \text{if } w_{\text{soil}}(t)z_{\text{soil}} < \theta_{\text{fc}}z_{\text{soil}} \\ (w_{\text{soil}}(t)-\theta_{\text{fc}})z_{\text{soil}}/\tau_{\text{soil}} & \text{if } w_{\text{soil}}(t)z_{\text{soil}} > \theta_{\text{fc}}z_{\text{soil}} \end{cases} \tag{3}$$

Where z_{soil} is the soil depth (mm) and τ_{soil} is a drainage coefficient in hours.

Matrix saturation occurs when the soil store becomes full. Water can only infiltrate as fast as the soil is draining, therefore matrix saturation excess becomes the input of water to the soil profile minus drainage:

$$q_{\text{sat}}(t) = \begin{cases} p_{\text{soil}}(t)-(\theta_{\text{sat}} - w_{\text{soil}}(t))/\tau_{\text{soil}} & \text{if } w_{\text{soil}}(t) + p_{\text{soil}}(t) > \theta_{\text{sat}} \\ 0 & \text{else} \end{cases} \tag{4}$$

Surface runoff can be generated two ways; saturation excess or infiltration excess. Therefore surface runoff (q_s) becomes the sum of infiltration excess (q_i) and matrix saturation excess (q_{sat}).

$$q_s(t) = q_{\text{sat}}(t) + q_i(t) \tag{5}$$

As the model is being applied on a storm event basis it is assumed that when rain is falling no evaporation takes place. The mass balance for soil water storage is accordingly given by:

$$\frac{dw_{\text{soil}}}{dt} = p_{\text{soil}}(t) - q_{ss}(t) - q_{\text{sat}}(t) \tag{6}$$

Title Page

Abstract | Introduction

Conclusions | References

Tables | Figures

◄◄ | ►►

◄ | ►

Back | Close

Full Screen / Esc

Printer-friendly Version

Interactive Discussion

EGU

which is similar to Woods (2003) except that evaporation is neglected in our case. Equations (1) to (6) are solved by discretizing Eq. (6) and the resulting system of algebraic equations are solved implicitly using a dynamic programming method in Mathematica 5.2 (Wolfram, 2005). To ensure that rainfall input into the rainfall partitioning model was at the same resolution (1.875 min), all input vectors had a length of 128 (240/1.875). Intensities at lower resolutions were repeated (time step (t^n) /1.875) times so that all vector lengths were the same.

Simulations were run for a clay, loam, sand and layered (duplex) soil for which the parameter values are listed in Table 1. Parameters for the saturated water content θ_{sat}, field capacity θ_{fc} and wilting point θ_{wp} were taken from Rawls et al. (1992). The drainage rate parameters τ_{soil} were order of magnitude estimates from saturated hydraulic conductivity for a 100 mm soil depth from Rawls et al. (1992). The infiltration capacity k_{soil} used were 12, 24 and 100 mm/h. This provided an order of magnitude range and a range of two orders of magnitude in the dimensionless analysis presented below. The layered soil, commonly referred to in Australia as a duplex soil, has a high infiltration capacity and a slower drainage due to an impeding layer. This was used as these soils are common in Australia and it allowed us to test the effect of changing the ratios of infiltration capacity and drainage rates. Simulations were run with initial conditions at field capacity and at wilting point.

2.2 Storm generation

Average storm properties used in the study are presented in Table 2. Total storm depth z_{storm} ranged from 1 to 600 mm with a storm duration t_{storm} of four hours. The mean intensities z_{storm}/t_{storm} ranged from 0.25 to 150 mm h^{-1} and were chosen to allow for a wide range of scaled parameters to be described later in this section. The storm duration was kept constant for scaling purposes but initial analysis of different durations shows the same patterns of results. Four hour storms represent approximate average storm durations in the south-west of Australia (Hipsey et al., 2003). This duration was long enough to investigate 6 cascades of rainfall resolutions (120, 60, 30, 15, 7.5, 3.75,

Sensitivity of runoff predictions to rainfall resolution

A. J. Hearman and C. Hinz

1.875 min) with the resolution halving at each cascade ($t_n=2^n t_0$) with $n=0, 1, 2, \ldots 6$ and $t_0=1.875$ min.

Rainfall intensities at these different resolutions were generated using the Bounded Random Cascade Model (Menabde and Sivapalan, 2000) parameterized to south-western Australian rainfall (Hipsey et al., 2003). Random cascades are based on the apparent multifractal scaling behaviour of rainfall. Rainfall variability at different time scales is determined by the analysis of break down coefficients which are defined as "the ratio of rainfall of a random field averaged over different scales where the smaller is contained within the larger" (Harris et al., 1998, pp. 93).

$$\mu(\tau, i) = \frac{R_\tau(t_n)}{R_i(t_n)} \quad \tau < i \tag{7}$$

Where $R_\tau(t_n)$ and $R_i(t_n)$ are the rainfall totals accumulated over the durations τ and i where τ is assumed to be completely included in the interval i (Menabde and Siva-palan, 2000). For a more detailed description of breakdown coefficients and their analysis see Harris et al. (1998). The probability distributions of the breakdown coefficients at different timescales characterize the variability of rainfall between successive temporal resolutions. Previous studies have shown scale dependence of variances of breakdown coefficients with time scales (Menabde et al., 1997 and Harris et al., 1998, Menabde and Sivapalan, 2000) with variances of breakdown coefficients decreasing with decreasing time scales. Figure 2 shows an example of a log-log plot of the α parameters of the beta distributions as a function of time resolution following a power law:

$$a(t) = a_0 t^{-H} \tag{8}$$

Rainfall is generated by starting with an initial homogeneous storm of a certain length (t_{storm}) and average storm intensity R_0. The next step is to divide the original storm duration (t_{storm}) into two halves and assign each half a value R_1 and R_2 where the sum of $R_1 t$ and $R_2 t=R_0 t$ and the weights at any level n, are drawn from the beta distribution

Sensitivity of runoff predictions to rainfall resolution

A. J. Hearman and C. Hinz

Title Page

Abstract	Introduction
Conclusions	References
Tables	Figures

◄◄ ►►

◄ ►

Back | Close

Full Screen / Esc

Printer-friendly Version

Interactive Discussion

EGU

with its sole parameter a estimated from the relationship (8). See Fig. 3 for an example of storm intensities generated for three different time scales (t). For further details on the generation of rainfall see Menabde and Sivapalan (2000).

An initial analysis of distributions of storms generated using the model was con-
ducted to determine a statistically stable number of storm realizations to be used in the analysis. The first, second and third moments were calculated for distributions of rain-fall intensities from x realizations of a storm event (x=25, 50, 100, 250, 500, 750, 1000, 2000). At x=500 the variations in the moments converged so that distributions with x values greater than 500 were not significantly different (T test, p=0.05) from x=500.
For this reason, five hundred realizations of each storm were used in the analysis.

2.3 Output analysis

The first, second and third moments of the distributions for infiltration excess, saturation excess, deep drainage and runoff were calculated for the amount (mm), time each process was active throughout the storm event (mins), frequency it was initiated and the maximum intensity ($mm\,h^{-1}$). The moments of the distributions of the scaled outputs were also calculated and used to compare the response of different soils to different storm properties.

2.4 Scaling of outputs

To determine the soil and rainfall conditions where model predictions of infiltration ex-
cess and saturation excess are most sensitive to rainfall resolution we scaled our model outputs and soil properties with average storm intensities. All model output intensities were multiplied by the time step and divided by the storm depth making them dimen-sionless. These dimensionless outputs were related to three dimensionless scaling parameters that were derived from three groups of dimensional parameters that char-
acterise the soil and the averaged rainfall properties. The soil parameters are the infil-tration capacity k_{soil} (Eq. 1) and the ratio of soil depth and drainage coefficient z_{soil}/τ_{soil}

(Eq. 3) controlling the drainage behaviour. The average rainfall is fully characterized by the average intensity z_{storm}/t_{storm}. All groups are rates in mm/h and ratios of these groups are used to carry out the scaling analysis presented below

Infiltration excess is produced when the supply of water (rainfall) exceeds the soil infiltration capacity threshold. By relating these two properties we can determine the amount of dimensionless infiltration excess for a range of infiltration capacities and average storm intensities using one curve. The scaling parameter we use to do this is k^* which is the ratio of maximum soil infiltration capacity to the average storm intensity.

$$k* = \frac{k_{soil}t_{storm}}{z_{storm}} \qquad (9)$$

The range of k^* values was 0.3 to 200 (see Table 2 for k^* values). The higher the average storm intensity relative to the infiltration capacity the smaller the k^* value.

Saturation excess occurs when the difference between the flux of water entering the soil and the flux of water leaving the soil (drainage) exceeds the soil storage capacity. The second dimensionless parameter, f^*, relates soil properties controlling the input of water (infiltration capacity, k_{soil}) to the soil properties controlling the output of water (z_{soil}/τ_{soil}):

$$f* = \frac{k_{soil}\tau_{soil}}{z_{soil}} \qquad (10)$$

The higher the infiltration rate multiplied by the drainage rate the deeper the soil required to maintain the same f^* value. The range of f^* values is presented in Table 1. The range of f^* parameters was limited to soil depths no shallower than 100 mm. For the sand, with a high infiltration capacity and fast drainage rate even at the shallowest soil depth (100 mm) no saturation excess was produced, making this the only depth simulated.

Now the soil properties that control saturation excess have been scaled (using f^*) we need to relate them to the storm properties that produce saturation excess. By doing

this we can determine the storm properties at which saturation excess is most sensitive to rainfall resolution for our range of f^* parameters. This was done by constructing the g^* parameter which is the average storm intensity in relation to the effective drainage rate.

$$g* = \frac{t_{storm}z_{soil}}{z_{storm}\tau_{soil}} = \frac{k*}{f*} \tag{11}$$

The f^* parameter ensures that the ratio of soil depth to drainage rate (effective drainage rate) is already scaled against the soil infiltration capacity so the g^* parameter relates this to changing average storm intensities.

3 Results and discussion

3.1 Model output

The rainfall resolution influences the amount and dynamics of infiltration excess and saturation excess runoff predictions. Figure 4 is an example of the model output for a single storm event showing two different rainfall resolutions; 1.875 min (black line) and 120 min (broken line). From this figure it can be seen that the higher resolution rainfall has higher peaks in intensities than the low resolution rainfall. This leads to infiltration excess being triggered in the high resolution rainfall input and no infiltration excess triggered with the low resolution rainfall. As a result more water is able to enter the soil for the low resolution rainfall and the soil is saturated for a longer period of time.

Figure 4 demonstrates that not only are the processes that generate runoff different for the two different rainfall resolutions but also the dynamics of runoff produced from different rainfall resolutions. High resolution rainfall generates more runoff with higher peaks in intensity. From this example we illustrate that rainfall resolution has a direct impact on the triggering of thresholds, in particular, infiltration excess. Models using time averaged rainfall would need to calibrate this threshold to a lower effective k_{soil}

Sensitivity of runoff predictions to rainfall resolution

A. J. Hearman and C. Hinz

Title Page

Abstract | Introduction

Conclusions | References

Tables | Figures

◄ | ►►

◄ | ►

Back | Close

Full Screen / Esc

Printer-friendly Version

Interactive Discussion

if they are to fit their model predictions to field measurements. However, even if the model is able to be calibrated to give the correct infiltration excess amount, using low resolution rainfall will give different dynamics. Low resolution rainfall will lead to long, low intensity predictions of runoff, whereas high resolution rainfall will lead to short, more intense bursts of runoff.

Whilst Fig. 4 is an example of one storm realization, the results presented in the sections that follow consider the statistical properties of the response, in particular the means of the distributions produced from 500 of these realizations.

3.2 Infiltration excess

3.2.1 Amounts

Using low rainfall resolution under predicts infiltration excess. This under prediction of infiltration excess can be seen in Fig. 5a where the high resolution rainfall of 1.875 min (n=0) produces more infiltration excess than the low resolution rainfall of 120 min (n=6). This figure also demonstrates that for different k^* values, the slopes of these curves, or the sensitivity to rainfall resolution are different. The sensitivity of predicted amounts of infiltration excess is summarized in Fig. 5b which shows the differences in infiltration amounts between 1.875 min resolution and 120 min resolution, which is the first point minus the last point for each curve in Fig. 5a. It can be seen that the scaling allows the curves for all soil types to collapse. They are most sensitive to rainfall resolution when the soil infiltration rate is 1.5 times the average storm intensity (ln k^*=0.4), where the amount of infiltration excess is under predicted by 25% of the total storm amount.

This supports Bronstert and Bardossy (2003) study who also found that the sensitivity of predictions of infiltration excess to rainfall resolution were highest where the average rainfall intensity was in the same order of magnitude as the infiltration capacity of the soil. It also gives us confidence that our simple threshold for infiltration excess produces similar results to a more complicated Darcian infiltration model used by Bronstert and Bardossy (2003).

Sensitivity of runoff predictions to rainfall resolution

A. J. Hearman and C. Hinz

Title Page

Abstract | Introduction

Conclusions | References

Tables | Figures

◄ | ►

◄ | ►

Back | Close

Full Screen / Esc

Printer-friendly Version

Interactive Discussion

EGU

Analysis of differences between smaller time steps (than our maximum 120 min) and our smallest timestep (1.875 min) show that the biggest differences also occur at ln k^*=0.4. Using 15 min resolution (n=3) still under predicts infiltration excess by 20% and 3.75 min resolution (n=1) under predicts infiltration excess by 10% of the total

5   storm volume at ln k^*=0.4. This implies that at the point scale when the soil infiltration rate is near 1.5 times the average storm intensity the rainfall resolution will impact runoff predictions even at resolutions less than 5 min.

Figure 6 can be used to explain why the maximum difference in amount of infiltration excess is at ln k^*=0.4. It describes the three different stages of threshold triggering

10   depending on rainfall resolution. At ln k^* values greater then 2.5, neither the high resolution rainfall nor the low resolution rainfall intensities are high enough to trigger infiltration excess (Fig. 6c). Where ln k^* is between 2.5 and 0.4, increasing the intensity of the storm leads to an increase in the amount of infiltration excess triggered by the high resolution rainfall, whereas the low resolution rainfall intensities are not high

15   enough to trigger this threshold (Fig. 6b). Where ln k^* is less than 0.4, the dimensionless difference in infiltration excess amounts decreases. This is because at ln k^*=0.4, infiltration excess is first triggered in the low resolution rainfall (Fig. 6d). The amount of infiltration excess then increases more rapidly for the low resolution rainfall than for the high resolution rainfall. This is because the low resolution rainfall has longer time steps

20   so once these intensities begin to trigger the threshold they spend a longer period of time above the threshold. From Fig. 6d it can be seen that at ln k^*=0.4, the initial point at which the low resolution rainfall begins to trigger the threshold is the point where there is the biggest difference between the amounts of infiltration excess produced from the different rainfall resolutions. As a result the maximum differences between the

25   two resolutions also occurs at this point (Fig. 6e). The labels a, b, c on graphs d and e of Fig. 6 refer to the three different stages of threshold triggering initially outlined in this paragraph.

Sensitivity of runoff predictions to rainfall resolution

A. J. Hearman and C. Hinz

Title Page	
Abstract	Introduction
Conclusions	References
Tables	Figures
◄◄	►►
◄	►
Back	Close
Full Screen / Esc	

Printer-friendly Version

Interactive Discussion

3.2.2 Dynamics

Not only are the amounts of infiltration excess different according to rainfall resolution but also the dynamics of this form of runoff. To quantify this we can look at plots of the way the mean maximum intensities, the frequency infiltration excess is triggered and
5 the time infiltration excess is active change with changes in average rainfall intensity scaled against the infiltration threshold of the soil, k^* (Fig. 7).

    With the high resolution rainfall having much higher intensity peaks than the lower resolution rainfall, the maximum intensities of the infiltration excess produced by the high resolution rainfall is also much higher. The differences in maximum intensities for
10 infiltration excess can also be explained according to the stages of threshold triggering illustrated in Fig. 6. At ln k^* values greater then 2.5 neither resolution exceeds the threshold so maximum intensities for all resolutions is 0. At ln k^* values between 2.5 and 0.4 the high resolution rainfall exceeds the threshold and maximums increase with increasing storm intensities (decreasing k^* values), however the low resolution
15 rainfall does not exceed the threshold so the maximums for low resolution rainfall are still 0. Meaning the difference increases proportionally with the increasing maximums generated from the high resolution rainfall. At ln k^* values less than 0.4 both resolutions exceed the threshold and increases in rainfall intensity lead to proportional increases in maximum intensities so that the differences in maximums reach a maximum (Fig. 7a).
20   The frequency the threshold is triggered is always higher with the higher resolution rainfall. See Fig. 7b. For the 120 min rainfall the threshold can only be triggered once, the intensity is either above the threshold for the entire storm duration or half of the storm duration at ln k^* values less than 0.4. As the intensities of the high resolution rainfall vary far more, the infiltration threshold is crossed more times. The frequency
25 of the triggering of this threshold reaches a maximum when the variations in intensity start to "wiggle" above the threshold at ln k^*=−0.5.

    The low resolution rainfall has longer time steps, so when infiltration excess is being triggered by both resolutions (ln k^*<0.4), the time infiltration excess is active is longer

at low resolutions and smaller at higher resolutions (Fig. 7c). This can also be related to the stages of threshold triggering. When the high resolution rainfall is triggering the infiltration threshold and the low resolution rainfall is not (Fig. 6b) the high resolution rainfall spends a longer period of time above the threshold (positive difference).

5 But when both resolutions are triggering the threshold (Fig. 6a) the low resolution has longer time steps so spends a longer period of time above the threshold, hence the difference in time infiltration excess becomes negative (Fig. 7c).

These differences in dynamics means that even at rainfall intensities where the amounts of predicted infiltration excess are more similar (greater average storm inten-

10 sities and smaller k^*) the dynamics of different rainfall resolutions are still very different, with high resolution rainfall producing shorter more intense bursts of infiltration excess. This has implications for the prediction of further threshold controlled processes such as erosion. It also influences the dynamics of this runoff further down the slope and whether it is able to reinfiltrate as runon or not. Wainwright and Parsons (2002) showed

15 that variable rainfall intensities results in a decrease in the runoff coefficient down slope with increasing slope length which does not occur when constant rainfall intensities are used.

3.3 Saturation excess

3.3.1 Amounts

20 Our simulations indicate that for soils with a saturated drainage rate greater than 5 times the infiltration capacity, $f^* \leq 0.2$, no saturation excess is triggered by either rainfall resolution. That is, fast draining and/or deep soils are not likely to produce saturation excess. This means for the fast draining sand tested, with $f^*=0.2$, even at a shallow soil depth of 100 mm no saturation excess was produced from either rainfall resolution.

25 These findings enabled us to split our soil into two groups, those susceptible to saturation excess with f^* values greater than 0.2 (which will be presented in this section) and those not susceptible to saturation excess with f^* values equal or less than 0.2.

EGU

Using low resolution rainfall in soils with f^* values greater than 0.2 can result in either an over prediction of saturation excess or an under prediction depending on the soil-storm relationships. Figure 8 shows how the amount of predicted saturation excess changes with different rainfall resolutions (x-axis) and with different storm intensities (various k^* values). The figure illustrates that for high rainfall intensities (low k^* values) that a low resolution rainfall predicts more saturation excess than at high resolutions. As we decrease the average intensity of the storm (increase the k^* value) this difference becomes smaller to a point where the high resolution rainfall predicts more saturation excess then the low resolution rainfall.

This change from an over prediction of saturation excess to an under prediction of saturation excess when using low resolution rainfall can be explained by changes in the temporal dynamics of the soil water storage in terms of different stages of threshold triggering (Fig. 9). In Fig. 9a, more saturation excess is predicted from the low resolution rainfall as the high constant intensity results in constant saturation excess. In contrast, the high resolution rainfall with variable intensities also has periods of low intensity where saturation excess is not triggered and the soil is able to drain so that the water content falls below the soil storage capacity. At storms of this intensity, infiltration excess is also being triggered by both rainfall resolutions, but the high resolution rainfall has more infiltration excess so less water is able to enter the soil than for the low resolution rainfall. In Fig. 9b, both resolutions trigger the threshold but because the low resolution rainfall is not losing any water to infiltration excess and has longer time steps, when it does trigger the threshold it spends more time above the threshold and the predicted saturation excess increases more rapidly than the high resolution rainfall (illustrated by the steeper curve of the low resolution rainfall in Fig. 9e). In Fig. 9c neither resolution is triggering the infiltration excess threshold so the saturation excess threshold can be triggered by the high resolution rainfall with bigger peaks in intensity and not the low resolution rainfall resulting in a positive difference in Fig. 9f. Low intensity storms where neither rainfall resolution triggers the threshold results in no difference in rainfall resolutions as illustrated in Fig. 9d.

Sensitivity of runoff predictions to rainfall resolution

A. J. Hearman and C. Hinz

Title Page

Abstract	Introduction
Conclusions	References
Tables	Figures

◄◄	►►
◄	►
Back	Close

Full Screen / Esc

Printer-friendly Version

Interactive Discussion

These differences in predictions of saturation excess using 1.875 min rainfall and 120 min rainfall (i.e. the mean amount predicted using 1.875 min rainfall minus the mean amount predicted using 120 min rainfall) for different soil types and soil depths are shown in Fig. 10. From this graph it can be seen that the maximum difference in over predictions of saturation excess (where the differences are most negative) scale with k^* and occur at ln k^*=0.4. This is because this is the point where there is the biggest difference in predictions of infiltration excess and therefore the biggest difference in amount of water entering the soil. The low resolution rainfall has no infiltration excess at this point so more water is able to enter the soil and this leads to a greater prediction of saturation excess than that predicted using the high resolution rainfall.

The size of this difference depends on the ratio of infiltration capacity to saturated drainage rate, f^*, with higher f^* values (shallower soils relative to the infiltration capacity and drainage coefficient) resulting in bigger differences in predictions (more negative) of saturation excess. This is because less water is required to saturate the soil profile so more saturation excess is predicted from the same amount of water entering the soil profile and thus a bigger difference in predictions from different rainfall resolutions.

From Fig. 10a it can be seen that the maximums of the positive differences do not all occur at the same ln k^* value. This is because infiltration excess is not being triggered at such low intensity storms. Instead, the maximum differences depend on how fast the soil is draining in relation to how fast the water is entering the soil i.e. the g^* parameter. Figure 10b presents the differences in amounts of saturation excess according to changing g^* values. It can be seen that the maximums of the positive differences in saturation excess occur when the saturated drainage rate is 7.4 times the average storm intensity (ln g^*=2). This is the point where low resolution rainfall begins to trigger the storage capacity threshold.

From Fig. 10 it can be seen that the size of the negative differences clearly relate to the f^* values, but the positive differences are more variable. This can be explained by the scaling methods used. The scaling relates steady state conditions or the average storm intensity to soil properties, but it does not account for the variations in intensi-

Sensitivity of runoff predictions to rainfall resolution

A. J. Hearman and C. Hinz

Title Page

Abstract	Introduction
Conclusions	References
Tables	Figures

|◄ | ►|

◄ | ►

Back | Close

Full Screen / Esc

Printer-friendly Version

Interactive Discussion

EGU

ties throughout a storm when smaller time steps are used (higher resolution rainfall). Saturation excess is triggered when the difference between the rate of water entering the soil and the rate of water leaving the soil exceeds the storage capacity. The soil storage capacity is scaled relative to steady state infiltration and drainage rates and does not account for the variations in the rate of water entering the soil when high rainfall resolutions are used. When the rainfall intensity exceeds the infiltration capacity the water enters the soil at a constant intensity (equal to the infiltration capacity) and this is why the negative differences in saturation excess scale with the f^* parameter. However, when the rainfall intensity does not exceed the soil infiltration capacity and the input is high resolution rainfall the water enters the soil at variable intensities. But the scaling does not account for the range in the rates that water can enter the soil. For this reason, differences in amounts of saturation excess between high resolution rainfall and steady state conditions are different for the soil types simulated even though these soils have the same f^* and g^* scaling parameters. For example the clay soil, with a much slower drainage coefficient (larger τ_{soil}) requires a deeper soil (5 times) to have the same saturated drainage rate in relation to maximum infiltration rate than the loam soil. But the range of intensities entering the clay soil is only 0–12 mm h^{-1} in comparison to 0–24 mm h^{-1} of the loam. Meaning that the clay soil requires a higher average intensity storm relative to effective drainage (smaller g^* value) before the peaks in intensity are able to exceed the storage capacity. Figure 11 compares examples of the changes in soil water storage throughout a four hour storm of a loam soil (a) and a clay soil (b) with the same f^* and g^* parameters. It can be seen that the high resolution input for the loam is more variable than the high resolution input of the clay. The high resolution input of the loam reaches the storage capacity whereas the high resolution input of the clay does not. This can be further explained using Fig. 9e. For the clay soil the period when neither resolution triggers the threshold (Fig. 9d and Section d of 9e) is longer. The range of storm intensities that the high resolution rainfall triggers the storage threshold but the low resolution rainfall does not (Fig. 9c and Section c of 9e) is shorter and hence the maximum difference between resolutions (9d) is smaller for

the clay soil.

3.3.2 Dynamics

Differences in predictions of dimensionless maximum saturation excess using different rainfall resolutions scale according to ratios of maximum infiltration capacity and average storm intensity, k^*, and depend on the ratio of maximum infiltration capacity to saturated drainage rates, f^* (Fig. 12a). Maximum differences in saturation excess are limited by the rate at which water can enter the soil (infiltration capacity). The biggest differences occur when the high resolution rainfall first begins to trigger the infiltration capacity threshold. When rainfall intensities exceed the infiltration capacity, the water enters the soil at a constant rate equal to the infiltration capacity and this is why the differences in maximum intensities at high rainfall intensities become zero. Differences are biggest in the deeper, faster draining soils (higher f^* values) as the low resolution rainfall is quickly drained away whilst the high resolution rainfall with its peaks in high intensities are able to increase soil water storage over a short period of time and cause saturation excess. The limit in rate water can enter the soil (soil infiltration capacity) means that the differences in maximum intensities produced by different rainfall resolutions is less than half those of the differences in dimensionless maximum infiltration excess intensities (compare Fig. 7a to 12a). This means that when runoff is dominated by saturation excess, rainfall resolution has less effect on maximum intensities than when runoff is dominated by infiltration excess, where differences in rainfall resolution result in much larger differences in maximum intensities.

Differences in the frequency saturation excess is triggered using different rainfall resolutions scale according to ratios of saturated drainage rates to average storm intensities (g^*) and the size of the differences depend on the soil types or drainage coefficient (Fig. 12b). The reason why differences in frequency are bigger for faster draining soils was explained above and illustrated in Fig. 11. Variations in the differences for the three soil types is a result of different f^* values or soil depths.

Similarly, differences in predicted time saturation excess is active throughout a storm

A. J. Hearman and
C. Hinz

Title Page

Abstract | Introduction

Conclusions | References

Tables | Figures

◄ | ►

◄ | ►

Back | Close

Full Screen / Esc

Printer-friendly Version

Interactive Discussion

using different rainfall resolutions scale according to ratios of saturated drainage rates to average storm intensities (g^*) and the size of the differences depend on the soil types or drainage coefficient (Fig. 12c). Again, variations in the differences for the three soil types is a result of different f^* values or soil depths.

5   While the differences in maximum intensities of saturation excess are much less than for infiltration excess the differences in frequency infiltration excess and saturation excess is triggered and the differences in time both infiltration excess and saturation excess is active between resolutions is far more similar for the two different runoff processes. So although the differences in dynamics of saturation excess between

10 different rainfall resolutions is similar to those differences produced by infiltration excess using different rainfall resolutions, the differences in maximum intensities are far less, making saturation excess produced from the high resolution rainfall more sporadic and only slightly more intense.

3.4 Runoff

15 Total runoff is a combination of infiltration excess and saturation excess and is always under predicted by low resolution rainfall (Fig. 14). The biggest differences in runoff occur on soils where maximum infiltration capacities were equal to or less than 1/5th of the saturated drainage rates ($f^* \leq 0.2$), when no saturation excess is produced so all runoff can be attributed to infiltration excess. When f^* was greater than 0.2, saturation

20 excess starts to be produced and runoff becomes more sensitive to rainfall resolutions at lower intensity storms. The sensitivity of runoff to rainfall resolution scales by the ratio of saturated drainage rate and average storm intensity (g^*) and is most sensitive when the saturated drainage rate is 7.4 times greater than average rainfall intensity (ln g^*=2). The biggest differences in total runoff are the same as the biggest positive

25 differences in saturation excess. This is because at this point low resolution rainfall is not producing any runoff at all and high resolution rainfall is producing saturation excess runoff. At higher rainfall intensities (lower g^*), the difference in total runoff amounts is smaller, but this is because the low resolution rainfall is predicting saturation excess

[EGU](#)

A. J. Hearman and
C. Hinz

runoff, in contrast to the high resolution rainfall predicting more infiltration excess. So although the sensitivity of total amounts of runoff appears to be lower at high intensity storms (lower g^*) the processes that dominate runoff depend on rainfall resolution. This will not only affect the dynamics of predicted runoff (implications have been discussed
5   earlier in the paper) but also predicted amounts of water entering the soil and therefore predictions of soil moisture and drainage.

Figure 13 has been presented according to soil types. At f^*=0.2, where all runoff is attributed to infiltration excess, the differences in predictions for all soil types are the same. For f^* values greater than 0.2 the slower draining clay soil has smaller
10   differences than the faster draining loam and layered soils for reasons outlined in the saturation excess section. Thus, predictions of runoff, for all soils, are most sensitive to rainfall resolutions when all runoff is attributed to infiltration excess only. For soils also susceptible to saturation excess runoff, faster draining, shallower soils are more sensitive than slower draining deeper soils.

15   Our simulations indicate that the biggest changes in storage amount occur in deep, clay soils where the initial soil moisture is at wilting point. With low resolution rainfall there is more storage as more water enters the soil (less infiltration excess) so there is an accumulation of water in the soil store until it reaches field capacity. Perhaps the biggest difference with storage due to different rainfall resolutions are the dynamics with
20   low resolution rainfall leading to a longer predicted time that the soil remains saturated, whereas the high resolution rainfall only has short bursts of saturation excess so the time when the soil is saturated is less. This may have ecological implications and implications for predictions of hill slope instabilities.

Simulations were also run for initial soil moistures at wilting point. No results from this
25   have been presented as the initial soil moisture makes little difference to the differences in predicted amounts of saturation excess between high and low resolution rainfall.

4 Conclusions

This paper shows that the triggering of infiltration excess and saturation excess thresholds is sensitive to rainfall resolution under certain soil-storm relationships. To explain this sensitivity we begin by splitting our soils into two groups; those susceptible to
only infiltration excess and those susceptible to both infiltration excess and saturation excess. Soils only susceptible to infiltration excess were deep/and or fast draining, where the maximum infiltration capacity was equal to or less than 1/5th of the saturated drainage rate ($f^* \leq 0.2$). Total runoff sensitivity for these soils scale according to the maximum infiltration capacity relative to average storm intensity (k^*). Soils susceptible to both infiltration excess and saturation excess runoff are slower draining, shallower soils where the maximum infiltration capacity made relative to the saturated drainage rate (f^*) is greater than 0.2. The sensitivity of total runoff predictions (infiltration excess plus saturation excess) to rainfall resolution scale by relating the saturated drainage rate to the average storm intensity (g^*).

Predictions of infiltration excess runoff for all soils were sensitive to rainfall resolutions when the maximum infiltration capacity was approximately 12 times the average storm intensity (i.e. $k^* < \ln 2$). The maximum differences occur when the soil infiltration capacity was 1.5 times the average storm intensity ($\ln 0.4$). At this point, amounts of infiltration excess were under predicted by 25% when two hourly rainfall was used compared to 1.875 min rainfall for this climate. Under these conditions, for soils where all runoff was attributed to infiltration excess ($f^* \leq 0.2$), the biggest discrepancy in amounts of predicted runoff using different rainfall resolutions occurs.

In contrast, soils that are susceptible to both saturation excess and infiltration excess have smaller maximum differences and these differences scale by relating saturated drainage rates and average storm intensities (g^*). Differences in the amount of runoff predicted from different rainfall resolutions occur when saturated drainage rates were between 20 times the average storm intensities and equal to the average storm intensity ($\ln g^*$ 0 and 3). The maximum differences occur when the saturated drainage rate

EGU

is 7.4 times greater than average rainfall intensity (ln g^*=2). This sensitivity depends on the soil depths and drainage coefficient. Deeper, slower draining soils show less predicted differences than shallower faster draining soils. The difference in amount of predicted runoff between rainfall resolution decreases as storms become more intense and ln g^* decreases from 2. This is because the high resolution rainfall begins to trigger the infiltration excess threshold so that less water is able to enter the soil and more runoff is attributed to infiltration excess. So although there may appear to be little or no difference in amounts of runoff between rainfall resolutions at ln g^* values greater than 2 the processes producing runoff depend on the rainfall resolution.

This study not only suggests that under these conditions using low resolution rainfall will under predict the amount of runoff but it will also influence the processes generating this runoff and the dynamics of this runoff. Infiltration excess predicted from high resolution rainfall is short and intense, whereas saturation excess produced from low resolution rainfall is more constant and less intense. The dynamics of this runoff has implications for the prediction of further threshold controlled processes such as erosion. It may influence runoff dynamics further down the slope and whether it is able to reinfiltrate as runon or not. The next step of this research is to determine the affects of rainfall resolution on runoff prediction at larger scales, namely the hillslope, and also for other climates.

References

Beven, K.: Runoff generation in semi-arid areas, Chapter 3 in: Dryland Rivers, Hydrology and geomorphology of semi-arid channels, edited by: Bull, L. J. and Kirkby, M. J., John Wiley and Sons Ltd, Sussex, England, 2002.

Bronstert, A. and Bardossy, A.: Uncertainty of runoff modelling at the hillslope scale due to temporal variations of rainfall intensity, Phys. Chem. Earth, 28, 283–288, 2003.

Canfield, H. E. and Goodrich, D. C.: The impact of parameter lumping and geometric simplication in modelling runoff and erosion in the shrublands of southeast Arizona, Hydrol. Processes, 20(1), 17–35, 2005.

Farmer, D., Sivapalan, M., and Jothityangkoon, C.: Climate, soil and vegetation controls upon the variability of water balance in temperate and semiarid landscapes: Downward approach to water balance analysis, Water Resour. Res., 39(2), 1035–1055, 2003.

Harris, D., Menabde, M., Seed, A., and Austin G.: Breakdown coefficients and scaling properties of rain fields, Nonlinear Processes Geophys., 5, 93–104, 1998.

Hipsy, M. R., Sivapalan, M., and Menabde, M.: A risk-based approach to the design of rural water supply catchments across Western Australia, Hydrol. Sci., 48(5), 709–727, 2003.

Horton, R. E.: The role of infiltration in the hydrological cycle, Transactions of the American Geophysical Union, 14, 446–460, 1933.

Kirkby, M. J.: Modelling water erosion processes, in: Soil Erosion, edited by: Kirkby, M. J. and Morgan, R. P. C., John Wiley, New York, 183–216, 1978.

Kirkby, M. J., Bracken, L. J., and Shannon, J.: The influence of rainfall distribution and morphological factors on runoff delivery from dryland catchments in SE Spain, Catena, 62, 136–156, 2005.

Kirkby, M. J. and Cox, N. J.: A climatic index for soil erosion potential (CSEP) including seasonal and vegetation factors, Catena, 25, 333–352, 1995.

Lovejoy, S. and Schertzer, D.: Multifractals, cloud radiances and rain, J. Hydrol., 1–30, 2005.

Menabde, M. and Sivapalan, M.: Modeling of rainfall time series and extremes using bounded random cascades and Levy-stable distributions, Water Resour. Res., 36(11), 3293–3300, 2000.

Menabde, M., Harris, D., Seed, A., Austin, G., and Stow, D.: Multiscaling properties of rainfall and bounded random cascades, Water Resour. Res., 33(12), 2823–2830, 1997.

Mertens, J., Raes, D., and Feyen, J.: Incorporating rainfall intensity into daily rainfall records for simulating runoff and infiltration into soil profiles, Hydrol. Processes, 16, 731–739, 2002.

Milly, P. C. D.: Climate, interseasonal storage of soil water and the annual water balance, Adv. Water Resour., 17, 19–24, 1994.

Over, T. M. and Gupta, V. K.: A space-time theory of mesoscale rainfall using random cascades, J. Geophys. Res., 101, 26 319–26 331, 1996.

Rawls, W. J., Ahuga, L. R., and Brakensiek, D. L.: Estimating soil hydraulic properties from soils data, in: Indirect Methods for Estimating the Hydraulic Properties of Unsaturated Soils, edited by: van Genuchten, M. T., Leij, F. J., and Lund, L. J., University of California, Riverside, California, 329–340, 1992.

Struthers, I., Sivapalan, M., and Hinz, C.: Conceptual examination of climate-soil controls upon

Sensitivity of runoff predictions to rainfall resolution

A. J. Hearman and C. Hinz

Title Page

Abstract	Introduction
Conclusions	References
Tables	Figures

|◄ | ►|

◄ | ►

Back | Close

Full Screen / Esc

Printer-friendly Version

Interactive Discussion

EGU

rainfall partitioning in an open-fractured soil. I. Single storm response, Adv. Water Resour., in press, 2006.

Wainwright, J. and Parsons, A. J.: The effect of temporal variations in rainfall on scale dependency in runoff coefficients, Water Resour. Res., 38(12), 1271, 2002.

5 Woods, R.: The relative roles of climate, soil, vegetation and topography in determining seasonal and long-term catchment dynamics, Adv. Water Resour., 26, 295–309, 2003.

Veneziano, D., Bras, R. L., and Nuiemann, J. D.: Nonlinearity and self-similarity of rainfall in time and a stochastic model, J. Geophys. Res., 101, 26 371–26 392, 1996.

Title Page

Abstract	Introduction
Conclusions	References
Tables	Figures

◄◄   ►►

◄   ►

Back   Close

Full Screen / Esc

Printer-friendly Version

Interactive Discussion

EGU

Table 1. Soil parameters used for simulations.

	k_{soil} (mm/h)	τ_{soil} (h)	z_{soil} (mm)	θ_{wp} (-)	θ_{fc} (-)	θ_{sat} r (-)	f^* (-)
Clay	12	20	100	0.15	0.30	0.50	2.40
			240				1.00
			500				0.48
			900				0.27
			1200				0.20
			1300				0.18
Loam	24	2	100	0.10	0.25	0.45	0.48
			178				0.27
			240				0.20
			300				0.16
Sandy loam	100	1	100	0.05	0.20	0.40	1.00
			208				0.48
			370				0.27
			500				0.20
Sand	100	0.2	100	0.05	0.20	0.40	0.20

Table 2. Storm properties and dimensionless infiltration parameters for three soils simulated.

average rainfall intensity $R_0 = z_{storm}/t_{storm}$ (mm/h)	total depth z_{storm} (mm)	storm	duplex soil k^* (-)	loam k^* (-)	clay k^* (-)
150.00	600		0.67		
100.00	400		1.00		
75.00	300		1.33		
66.75	267		1.50		
50.00	200		2.00		
40.00	160		2.50	0.60	0.30
36.00	144		2.78	0.67	0.33
32.00	128		3.13	0.75	0.38
24.00	96		4.17	1.00	0.50
20.00	80		5.00	1.20	0.75
16.00	64		6.25	1.50	1.00
12.00	48		8.33	2.00	1.50
8.00	32		12.50	3.00	2.00
6.00	24		16.67	4.00	3.00
4.00	16		25.00	6.00	4.00
2.00	8		50.00	12.00	6.00
1.00	4		100.00	24.00	12.00
0.50	2		200.00	48.00	24.00
0.25	1				48.00

EGU

Precipitation (p_{rain})

Infiltration Capacity (k_{soil})

Matrix Infiltration (p_{soil})

Infiltration Excess (q_i)

Saturation (θ_{sat})   Saturation Excess (q_{sat})

Runoff (q_s)

Field Capacity (θ_{fc})

Soil depth (z_{soil})

Soil Matrix Store (w_{soil})

Matrix Drainage (q_{ss})
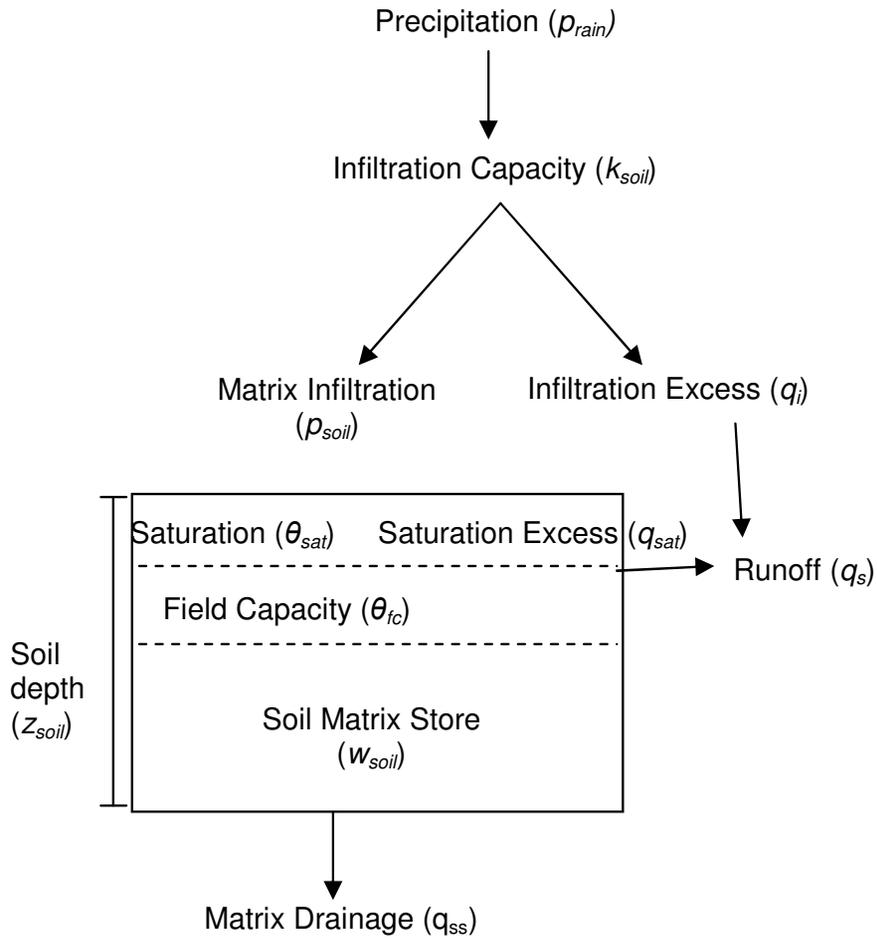
Fig. 1. Diagram of the conceptual bucket model.

EGU

Full Screen / Esc

Printer-friendly Version

Interactive Discussion

Fig. 2. Changes in alpha parameters of fits of the beta distributions to breakdown coefficients at different time scales.

EGU
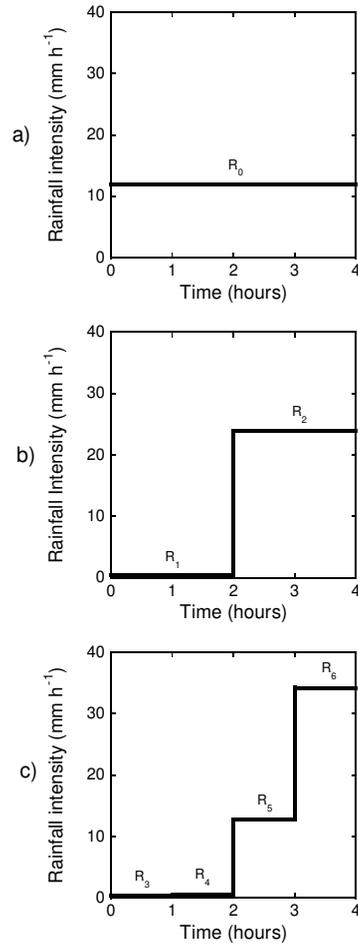
Fig. 3. Diagram of rainfall generation at cascading time steps (4 h, 2 h and 1 h).
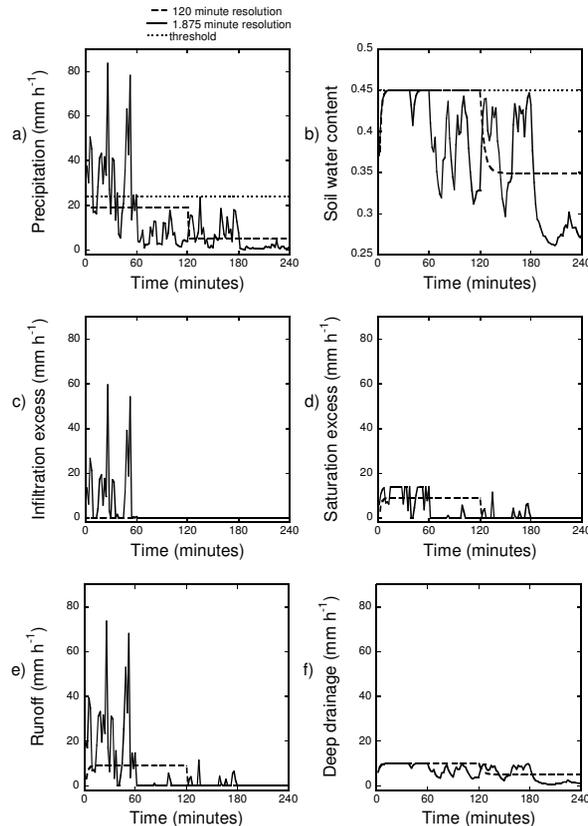
Fig. 4. Example of the model input (precipitation **(a)**) and model outputs (soil water content **(b)**, infiltration excess **(c)**, saturation excess **(d)**, runoff **(e)** and deep drainage **(f)**). Produced from one storm (48 mm) at two different rainfall resolutions (1.875 min and 120 min) for a loam soil with a depth of 100 mm.
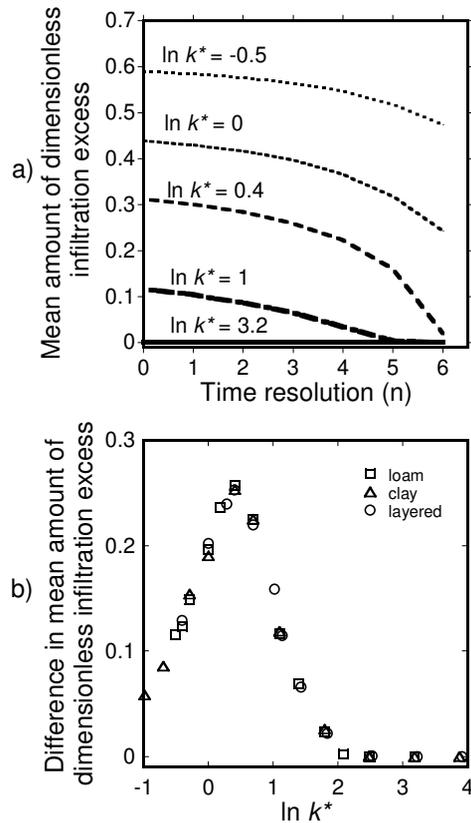
Fig. 5. (a) The changes in mean amount of dimensionless infiltration excess with the 7 different time resolutions tested ($n=0,1,2....6$, $t_n=2^n\,t_0$ where $t_0=1.875\,\text{min}$) for a loam soil at various mean rainfall intensities relative to the infiltration capacity (k^*). **(b)** The difference in mean dimensionless amount of infiltration excess between 1.875 and 120 min resolution according to changes in the natural log of k^* for the clay, loam and layered soils.
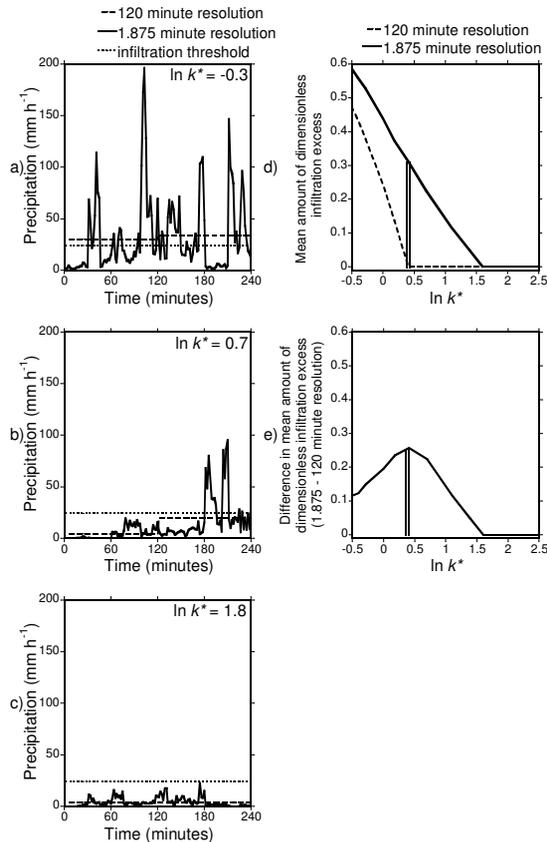
Fig. 6. Illustrates the effect that the different "stages" of infiltration excess threshold triggering (**(a)** both resolutions trigger the threshold, **(b)** the high resolution triggers the threshold and **(c)** neither resolution trigger the threshold) have on **(d)** the mean amount of infiltration excess for changing k^* for the different resolutions and therefore **(e)** the difference in amount of infiltration excess predicted from the two resolutions.

Sensitivity of runoff predictions to rainfall resolution

A. J. Hearman and
C. Hinz
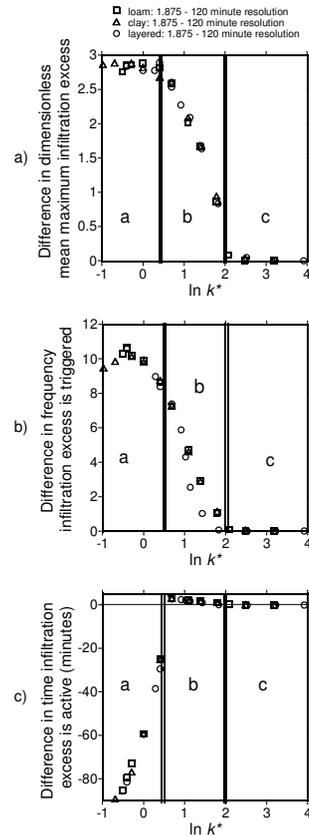
Fig. 7. The differences in **(a)** dimensionless maximum infiltration excess, **(b)** frequency infiltration excess is triggered and **(c)** time infiltration excess is active using 1.875 and 120 min resolutions, changing k^* values and clay, loam and layered soils. Sections a, b and c represent the different stages of threshold triggering illustrated in Fig. 6.
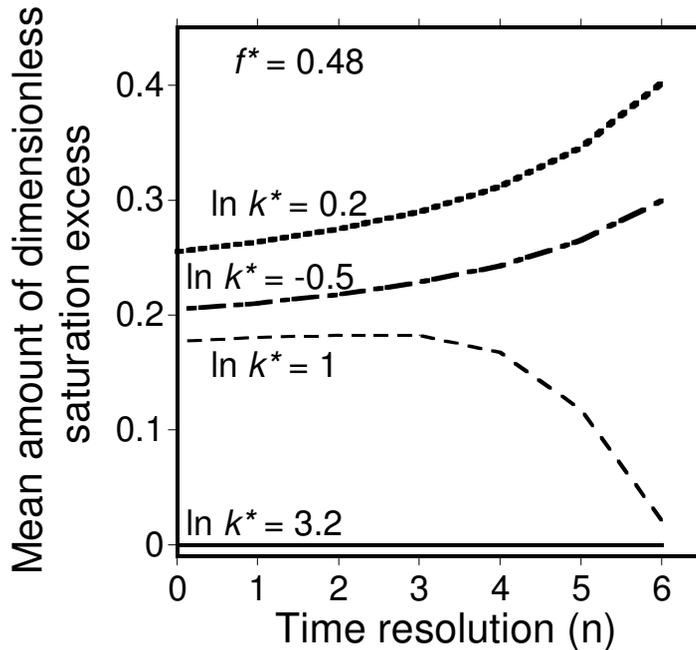
Fig. 8. The changes in mean amount of dimensionless saturation excess with the natural log of the 6 different time resolutions tested tested ($n=0,1,2\ldots6$, $t_n=2^n\,t_0$ where $t_0=1.875\,\text{min}$ for a loam soil with an initial water content at field capacity for storms with different mean rainfall intensities relative to the infiltration capacity (k^*).

EGU

Sensitivity of runoff predictions to rainfall resolution

A. J. Hearman and
C. Hinz

Title Page

Abstract | Introduction

Conclusions | References

Tables | Figures

◀◀ | ▶▶

◀ | ▶

Back | Close

Full Screen / Esc

Printer-friendly Version

Interactive Discussion
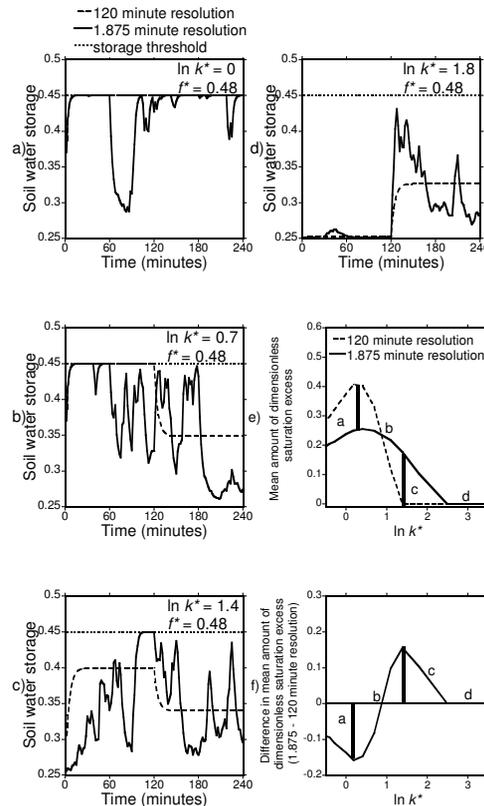
Fig. 9. Illustrates the effect that the different "stages" of saturation excess threshold triggering (**(a)** high intensity storms where the low resolution rainfall triggers saturation excess threshold throughout the whole storm, **(b)** both resolutions trigger the threshold, **(c)** only the high resolution triggers the threshold and **(d)** neither resolution triggers the threshold) have on **(e)** the mean amount of saturation excess for changing k^* for the different resolutions and therefore **(f)** the difference in amount of saturation excess predicted from the two resolutions.
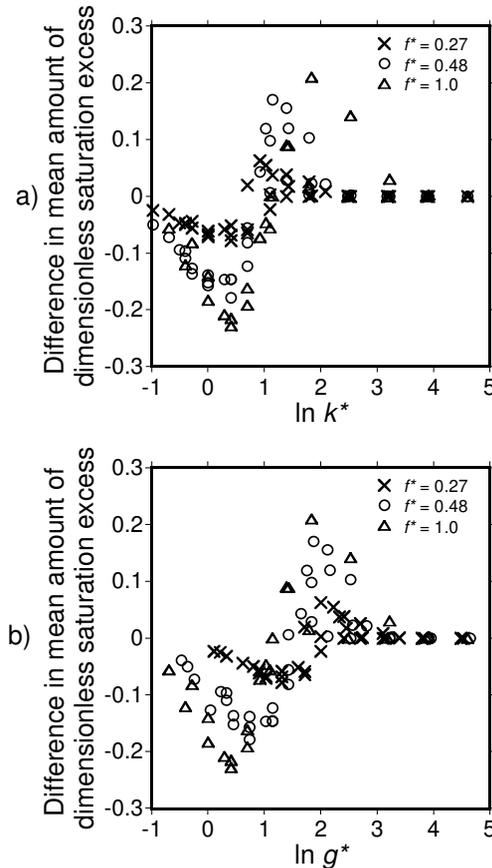
Fig. 10. The difference in mean dimensionless amount of saturation excess between 1.875 and 120 min resolution according to changes in **(a)** the natural log of k^* and **(b)** the natural log of g^* for the clay, loam and layered soils with f^* values of 0.27, 0.48 and 1 and initial soil water contents at field capacity.

EGU
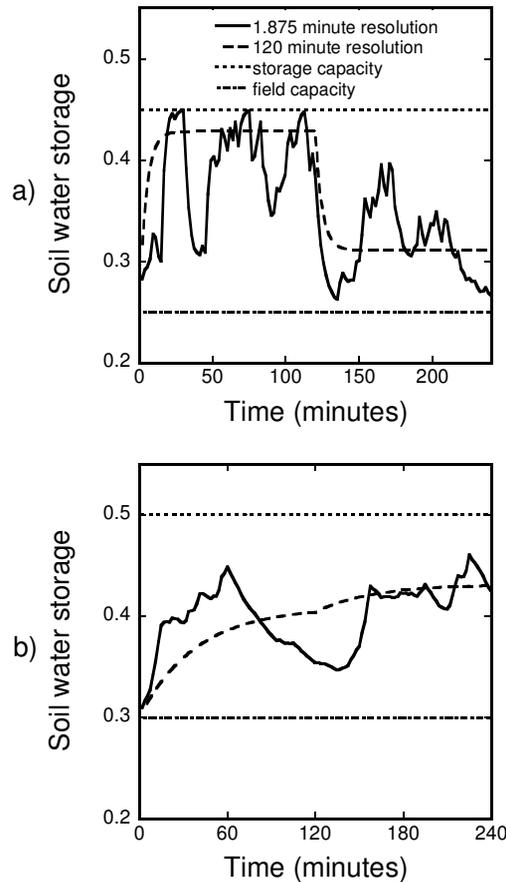
Fig. 11. The change in soil water storage throughout a single storm for **(a)** a loam soil and **(b)** a clay soil with the same g^* and f^* values (ln 2.4 and 0.48, respectively).

Title Page

Abstract | Introduction

Conclusions | References

Tables | Figures

|◄ | ►|

◄ | ►

Back | Close

Full Screen / Esc

Printer-friendly Version

Interactive Discussion

EGU
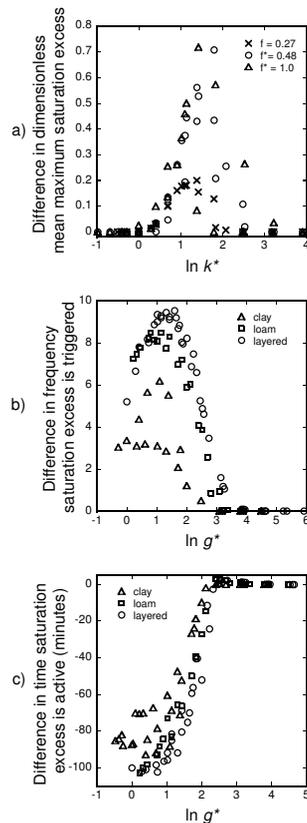
Fig. 12. The differences in **(a)** dimensionless maximum saturation excess for changing k^* values, **(b)** frequency saturation excess is triggered for changing g* values, and **(c)** time saturation excess is active for changing g* values, using 1.875 and 120 min resolutions, f^* values of 0.27, 0.48 and 1, and clay, loam and layered soils.
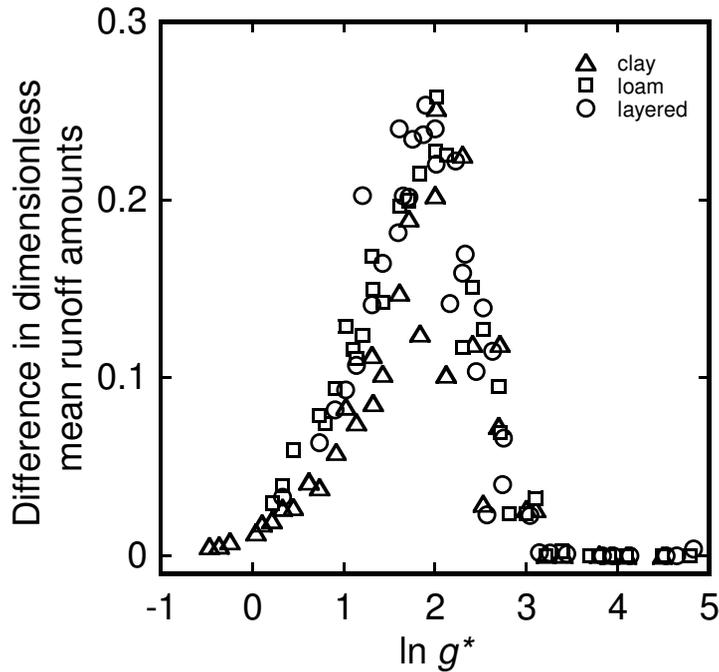
Fig. 13. The difference in dimensionless runoff between 1.875 and 120 min resolution according to the natural log of g^* for f^* values of 0.20, 0.27 and 0.48 for clay, loam and layered soils.